



Probabilistic fatigue life prediction using an equivalent initial flaw size distribution

Yongming Liu^{a,*}, Sankaran Mahadevan^b

^aClarkson University, P.O. Box 5710, 8 Clarkson Avenue, Potsdam, NY 13699, USA

^bVanderbilt University, Nashville, TN 37235, USA

ARTICLE INFO

Article history:

Received 20 February 2008

Received in revised form 18 June 2008

Accepted 20 June 2008

Available online 4 July 2008

Keywords:

Fatigue

Life prediction

Initial flaw

Crack growth

Reliability

ABSTRACT

A new methodology is proposed in this paper to calculate the equivalent initial flaw size (EIFS) distribution. The proposed methodology is based on the Kitagawa–Takahashi diagram. Unlike the commonly used back-extrapolation method for EIFS calculation, the proposed methodology is independent of applied load level and only uses fatigue limit and fatigue crack threshold stress intensity factor. The advantage of the proposed EIFS concept is that it is very efficient in calculating the statistics of EIFS. The developed EIFS methodology is combined with probabilistic crack growth analysis to predict the fatigue life of smooth specimens. Model predictions are compared with experimental observations for various metallic materials.

© 2008 Elsevier Ltd. All rights reserved.

1. Introduction

The fatigue crack growth (FCG) process is stochastic in nature. Life prediction and reliability evaluation are critical for the design and maintenance planning of many structural components, but are still challenging problems despite extensive research during the past several decades. Two major types of methodologies are available for fatigue life prediction. One type is based on material $S-N$ (or $\epsilon-N$) properties and a damage accumulation rule. The other type is based on fracture mechanics and crack growth analysis, which is the physical basis for damage tolerance analysis. One problem in the fracture mechanics-based life prediction is to determine the initial crack size for crack growth analysis. One practice is to use an empirically assumed crack length, such as 0.25–1 mm for metals [1–3]. An alternative way is to use results from nondestructive inspection (NDI) [4]. However, the initial flaw size (IFS) can be below the current detection capability of the NDI technique. If the NDI detection limit is chosen as the initial flaw size, it will result in a very conservative design [5]. Other approaches have used experimentally measured defect size and shape for crack growth analysis. Merati and Eastaugh [3] used experimental study to investigate the initial discontinuity state (IDS) for 7000 aluminum alloys, which can be used for fatigue modeling purpose.

The equivalent initial flaw size (EIFS) concept was developed nearly 30 years ago in an attempt to determine the initial crack size for fracture mechanics-based life prediction. The EIFS accounts for the initial quality, both from manufacturing and bulk material

properties of structural details. The calculation of EIFS is usually performed using a back-extrapolation method. This approach uses fatigue crack growth analysis with an assumed initial crack geometry and size to match the material failure data (stress-life). The initial crack size is obtained by trial and error method and is named as EIFS. Yang and Manning [6] used this back-extrapolation technique to obtain the EIFS distribution of Al 2024-T351. White et al. [7] used a probabilistic fracture approach to derive the equivalent pre-crack size (EPS), which is also based on the back-extrapolation method. Molent et al. [8] used a back projection of the experimental crack growth curve to time zero to derive the EPS for Al 7050. The major problem using the back-extrapolation method is that the obtained EIFS seems to be dependent on stress level [9]. It is desirable to view EIFS as a material property indicating the initial quality of the material and not connected to the applied stress level; this would make the EIFS applicable to a wide range of stress levels.

However, it should be noted that EIFS is not a physical quantity. It is a quantity extrapolated from experimental data simply to facilitate life prediction by using only long crack growth analysis and avoiding the difficulties of short crack growth modeling.

Widespread use of EIFS concept has not been realized due to the large amount of test data required to develop a reliable EIFS distribution [10]. When the uncertainties associated with EIFS need to be included, the problem becomes more complicated. Due to the inherent variability of fatigue crack growth data, failure data, and also the modeling approximations in the fatigue crack growth (FCG) analysis, the uncertainties of EIFS need to be carefully accounted for in probabilistic life prediction. The back-extrapolation method makes the computation of probabilistic EIFS distribution

* Corresponding author. Tel.: +1 315 268 2341; fax: +1 315 268 7985.
E-mail address: yliu@clarkson.edu (Y. Liu).

very expensive, because Monte Carlo simulation is usually coupled with iterative fatigue crack growth analysis [11,12]. Thus there is a need for an accurate and efficient calculation methodology to construct the probability distribution of EIFS.

A new probabilistic EIFS calculation methodology based on the Kitagawa–Takahashi diagram is proposed in this paper. The EIFS is determined by matching the infinite life of a component with and without an assumed initial crack. The proposed methodology only uses fatigue limit data and fatigue crack threshold stress intensity factor. The statistics of EIFS are directly calculated without solving inverse fatigue crack growth analysis. A probabilistic fatigue crack growth analysis using the proposed EIFS calculation is used to predict the fatigue life of smooth specimens under constant amplitude cyclic loading. Model predictions are compared with experimental data for various metallic materials.

2. EIFS calculation

2.1. Basic concept of the proposed EIFS

A straightforward way to predict material/component fatigue life using the fracture mechanics-based approach is to perform the fatigue crack growth analysis starting from the actual initial flaw, such as interval voids and nonmetallic inclusions. For materials with large initial flaws, the actual initial flaw size can be combined with long crack $da/dN \sim \Delta K$ relationship to predict fatigue life. However, most metallic materials have initial flaws with length scale smaller than the micro-structural features such as average grain size. Fatigue crack growth behavior of a micro-structural small crack differs significantly from that of a long crack [13]. A schematic plot of long crack and small-crack growth curves is shown in Fig. 1. The long crack growth rate exhibits an asymptotic behavior as the crack becomes smaller and smaller, i.e. crack threshold. The small-crack growth rate for the same ΔK value is several times faster than those predicted by long crack growth data. Lankford and Hudak [13] compared the anomalous behavior of ‘small’ fatigue crack growth behavior with that of long crack for nickel-based alloys. Kaynak et al. [14] compared the anomalous initiation and growth behavior of small cracks in steel and evaluated the effect of grain size. Small-crack growth data usually does not have the monotonic trend as that of the long crack growth data and shows oscillatory behavior [15], which is believed to be caused by micro-structural barrier effects, such as grain boundaries. Some recent studies used micro-mechanics and crystal plasticity for small-crack analysis [16–18]. A comprehensive review of the small-crack growth behavior is not the focus of this study and an overview of small-crack growth can be found in [19]. Some fatigue life prediction methods using small-crack growth theory and actual initial flaw size have been proposed in the literature [3,20,21]. One difficulty with this type of approach is that the

mechanism of small-crack growth has not been fully understood. The other difficulty is that small-crack growth strongly depends on the material microstructure and has very large uncertainties caused by randomness of grain size, grain orientation and initial flaw shape. This causes additional difficulties for probabilistic life prediction. In order to overcome such difficulties, the EIFS concept avoids small-crack growth analysis and instead uses an equivalent initial flaw size in long crack growth analysis that would match the fatigue life of specimens.

Fatigue life prediction is performed by integration of the fatigue crack growth rate curve. A general fatigue crack growth rate curve can be expressed as

$$da/dN = f(\Delta K), \tag{1}$$

where f is a function used to describe the relationship between da/dN and ΔK , such as the Paris law for linear regime and other type of functions to include crack growth for near-threshold crack growth and unstable crack growth (Fig. 1). Under constant amplitude loading $\Delta\sigma$, Eq. (1) can be expressed as

$$da/dN = g(a) \tag{2}$$

and fatigue life can be obtained as

$$N = \int_0^N dN = \int_{a_i}^{a_c} \frac{1}{g(a)} da, \tag{3}$$

where a_i is the initial crack length. a_c is the critical length at failure and can be calculated using fracture toughness and applied load. Considering the actual initial flaw size (IFS) and including the small-crack growth curve $g_s(a)$, fatigue life N_{IFS} is obtained as

$$N_{IFS} = \int_{IFS}^{a_c} \frac{1}{g_s(a)} da. \tag{4}$$

Considering equivalent initial flaw size (EIFS) and using only a long crack growth curve $g_l(a)$, fatigue life N_{EIFS} is obtained as

$$N_{EIFS} = \int_{EIFS}^{a_c} \frac{1}{g_l(a)} da. \tag{5}$$

A schematic plot of using these two approaches is shown in Fig. 2. It is shown that both approaches can give the same life prediction if the EIFS is properly chosen and the underlying areas below $g_s(a)$ and $g_l(a)$ are equal. The key idea in the proposed approach is to avoid the calculation using small-crack growth $g_s(a)$. Thus, instead of matching life predictions between long crack growth and small-crack growth analysis, we calculate the EIFS by matching the life prediction of long crack growth analysis with that observed in fatigue S–N testing because rigorous small-crack growth analysis should give the same life value. Theoretically speaking, any experimental fatigue-life data under arbitrary constant amplitude load can be used to calculate EIFS, which is the approach used by the

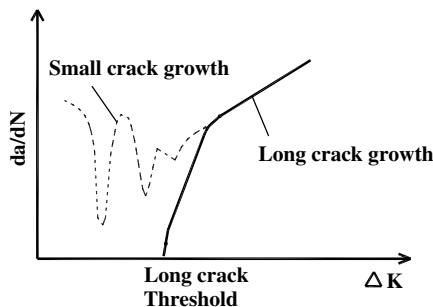


Fig. 1. Schematic illustration of small crack and long crack growth.

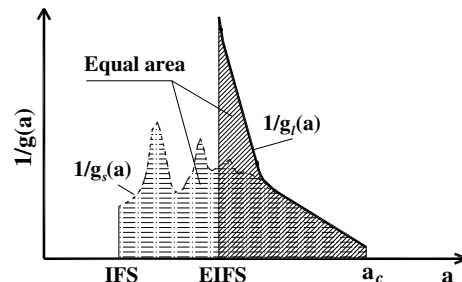


Fig. 2. Schematic illustration of actual initial flaw size and EIFS using long crack growth.

commonly used back-extrapolation method. In this paper, we calculate the EIFS by matching the infinite fatigue life obtained from Eq. (5) with the experimental data from S–N tests, i.e.

$$N_{\text{EIFS}} = \int_{\text{EIFS}}^{\sigma_c} \frac{1}{g_i(a)} da \rightarrow +\infty \quad \text{when} \quad \Delta\sigma \rightarrow \Delta\sigma_f, \quad (6)$$

where $\Delta\sigma$ is the applied stress range and $\Delta\sigma_f$ is the fatigue limit (fatigue strength at the infinite fatigue life) observed from S–N testing. As shown in Eq. (6), the value of EIFS will affect the integration results and the life prediction. For a certain value of the EIFS, the integration is infinity due the asymptotic behavior of the long crack growth curve, which matches the observed life from S–N testing. The details of the calculation of the EIFS by matching the infinite life are shown in Section 2.2.

It is noticed that the structural integrity is usually controlled by the largest flaw. These largest flaws may come from manufacturing (e.g., large initial voids or inclusions) or from operation activities (e.g., surface scratches due to maintenance). This study aims to develop a general methodology for EIFS determination under well controlled laboratory environments (e.g. good surface polishing of smooth specimens). Proper modifications are required to extend the proposed methodology to structural level integrity assessment, where the large flaw in realistic situation will be included. One such example can be found in [22] by the same authors, where a bi-modal distribution was used to capture the effect of the largest flaw on the fatigue reliability assessment of railroad wheels. It is found that the right tail distribution has a large effect on the fatigue reliability estimation. In the current investigation, the experimental data collected only contains 3–5 data points for threshold stress intensity factor estimation and is not sufficient to investigate the tail shape effect on the probability estimation.

2.2. Deterministic EIFS calculation

To match the infinite fatigue life, the concepts of fatigue limit and fatigue crack threshold stress intensity factor are used here. The concept of fatigue limit is traditionally used within the safe-life design approach, which defines a loading criterion under which no failure occurs. The concept of fatigue crack threshold is often used within the damage tolerance design approach, which defines a loading criterion under which the cracks will not grow significantly. A link between the traditional safe-life design approach and damage tolerance design approach has been proposed and known as the Kitagawa–Takahashi (KT) diagram [23]. A schematic plot of the KT diagram is shown in Fig. 3. According to the KT diagram, the fatigue limit of the cracked specimen increases as the crack size decreases. The fatigue limit of the cracked specimen re-

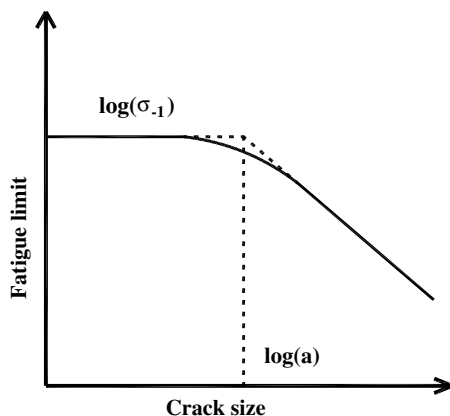


Fig. 3. Schematic representation of the Kitagawa–Takahashi diagram.

mains constant when the crack size is below a certain value, which is determined by fatigue limit of the material (i.e., the value from smooth specimen testing) and the fatigue crack threshold intensity factor using linear elastic fracture mechanics (LEFM). El Haddad et al. [24] proposed a model to express the fatigue limit $\Delta\sigma_f$ using the fatigue threshold stress intensity factor ΔK_{th} and a fictional crack length a

$$\Delta K_{\text{th}} = \Delta\sigma_f \sqrt{\pi a} Y, \quad (7)$$

where Y is a geometry correction factor and depends on the crack configuration. For an infinite plate with a centered through crack of length $2a$, Y is unity. For other crack configurations, Y can be obtained from stress intensity factor solutions available in the literature [25].

Eq. (7) is rewritten as

$$a = \frac{1}{\pi} \left(\frac{\Delta K_{\text{th}}}{\Delta\sigma_f Y} \right)^2. \quad (8)$$

Eq. (8) is the expression for the proposed EIFS. If the specimen has an initial crack length of EIFS and is under the stress range $\Delta\sigma_f$, the calculated fatigue life using a fracture mechanics-based approach is infinity (Eq. (5)), which is the experimental fatigue life under fatigue limit.

From Fig. 2, it is seen that the proposed EIFS includes the effect of actual flaw size and small-crack growth behavior. This information is implicitly included in material properties $\Delta\sigma_f$ and ΔK_{th} . For example, suppose we have two materials A and B, which have exactly the same crack growth behavior and threshold stress intensity factor. Material A has very small actual flaw size, and thus a large proportion of small-crack growth. Material B has very large actual initial flaw size, and thus a small proportion of small-crack growth. Material A will have a higher fatigue limit compared to material B since the latter has larger defects. From Eq. (8), we know that the EIFS for material A is larger than the EIFS for material B. The proposed EIFS is smaller if the material has a large proportion of small-crack growth. And the portion of small-crack growth can be implicitly reflected by the ratio of ΔK_{th} and $\Delta\sigma_f$.

Another concern in using the proposed EIFS is the assumed crack configuration. From Eq. (8), it is seen that the EIFS not only depends on material properties $\Delta\sigma_f$ and ΔK_{th} , but also depends on the geometry correction factor Y . If different initial crack configurations are assumed, the calculated EIFS is different. Two configurations are explored in this paper for smooth plate specimens. One is center-through crack and the other is surface crack. A schematic plot is shown in Fig. 4 for these two configurations.

The geometry correction factor for a center-through crack of finite width plate can be expressed as [25]

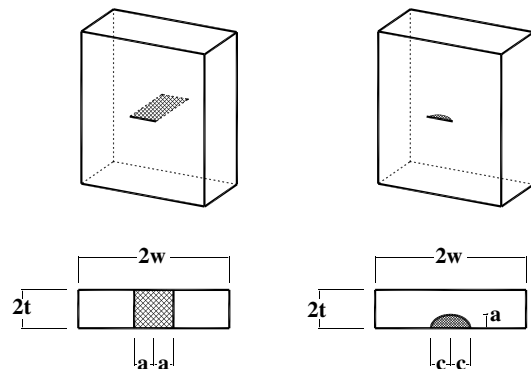


Fig. 4. Schematic representation of center-through crack and semi-elliptical surface crack.

$$Y = \left[\sec\left(\frac{\pi a}{2W}\right) \right]^{\frac{1}{2}}, \tag{9}$$

where $2a$ is the crack length and W is the plate width.

The geometry correction factor for a surface crack can be expressed as [25–27]:

$$Y = \left[\frac{\left(\sin^2 \phi + \left(\frac{a}{t}\right)^2 \cos^2 \phi \right)^{\frac{1}{4}}}{E(k)} \right] M_f, \tag{10}$$

where a is the depth and $2c$ is the surface length of a semi-elliptical flaw. The term in square brackets represents the solution of the equivalent embedded elliptical flaw. The parameter ϕ is the angle in the parametric equation of ellipse and $E(k)$ is a complete integral of the second kind [26]. The correction factor M_f for finite width W and finite thickness t is calculated as

$$M_f = (M_1 + M_2 \left(\frac{a}{t}\right)^2 + M_3 \left(\frac{a}{t}\right)^4) g f_w, \tag{11}$$

where

$$M_1 = 1.13 - 0.09 \frac{a}{c},$$

$$M_2 = -0.54 - \frac{0.89}{0.2 + \frac{a}{c}},$$

$$M_3 = 0.5 - \frac{1}{0.6 + \frac{a}{c}} + 14 \left(1 - \frac{a}{c}\right)^{24},$$

$$g = 1 + \left(0.1 + 0.35 \left(\frac{a}{t}\right)^2\right) (1 - \sin \phi)^2,$$

$$f_w = \sec\left(\frac{\pi c}{2W} \sqrt{\frac{a}{t}}\right).$$

In the current study, the surface flaw is assumed to be semi-circular in shape, i.e. $a/c = 1.0$. The stress intensity factor solution at the surface crack tip ($\phi = 0$) is used for the EIFS calculation. It should be noted that surface crack growth is actually a 3D crack problem, where the crack front experiences complicated crack growth behavior. In the current study, only crack growth at the surface crack tip is considered and more complex situations need further study.

The traditional EIFS methodology uses back-extrapolation method to calculate the EIFS distribution. If the fatigue S–N testing data under different stress levels are used for extrapolation (constant amplitude loading), different EIFS distributions are obtained, which makes the EIFS distribution stress level dependent [10]. In the proposed method, the EIFS is determined by KT diagram and not by data from multiple stress levels. Thus, the proposed EIFS is independent of stress levels by definition.

2.3. Probabilistic distribution of EIFS

The above discussion is for deterministic calculation of EIFS. One of the advantages of the proposed EIFS methodology is that it makes it very convenient to calculate the probabilistic distribution of EIFS.

Different types of probabilistic distributions have been used in the literature to describe the EIFS distribution, such as the lognormal, Weibull and three parameter Weibull distributions [11,12,28]. In Eq. (8), since both the fatigue limit and fatigue crack threshold stress intensity factor are random variables, EIFS is also a random variable. In this study, lognormal distributions are assumed for the fatigue limit and fatigue crack threshold stress intensity factor. Thus, EIFS also become a lognormal random variable. This assumption makes the calculation of the statistics of EIFS very efficient. The statistics, i.e. mean and standard deviation, of the fatigue limit

(μ_1 and σ_1) and fatigue crack threshold stress intensity factor (μ_2 and σ_2) can be obtained from experimental data. The objective is to calculate the mean and standard deviation of EIFS (μ and σ). Eq. (8) can be rewritten in logarithmic form as

$$\log(a) = -(\log(\pi) + \log(Y)) + 2 \log(\Delta K_{th}) - 2 \log(\Delta \sigma_f). \tag{12}$$

EIFS is usually very small compared to the width and thickness of the specimen. Thus, the geometry correction factor can be simplified. For a center-through crack in a plate, $Y = 1$. For surface crack in a plate, $Y = 2.24/\pi$ (stress intensity factor solution for a semi-circular flaw in semi-infinite plate). The first term in Eq. (12) is a constant. Since $\Delta \sigma_f$ and ΔK_{th} are lognormal random variables, $\log(\Delta K_{th})$ and $\log(\Delta \sigma_f)$ are Gaussian random variables. The mean and standard deviation of $\log(\Delta K_{th})$ can be calculated as

$$\begin{cases} \mu_{1L} = 2 \log(\mu_1) - \frac{1}{2} \log(\mu_1^2 + \sigma_1^2) \\ \sigma_{1L} = [-2 \log(\mu_1) + \log(\mu_1^2 + \sigma_1^2)]^{\frac{1}{2}} \end{cases} \tag{13}$$

Similarly, the mean and standard deviation of $\log(\Delta \sigma_f)$ can be calculated as

$$\begin{cases} \mu_{2L} = 2 \log(\mu_2) - \frac{1}{2} \log(\mu_2^2 + \sigma_2^2) \\ \sigma_{2L} = [-2 \log(\mu_2) + \log(\mu_2^2 + \sigma_2^2)]^{\frac{1}{2}} \end{cases} \tag{14}$$

The mean and standard deviation of $\log(a)$ can be calculated based on Eq. (12) as

$$\begin{cases} \mu_L = -\log(\pi) - \log(Y) + 2(\mu_{1L} - \mu_{2L}) \\ \sigma_L = 2[\sigma_{1L}^2 + \sigma_{2L}^2 - 2\rho\sigma_{1L}\sigma_{2L}]^{\frac{1}{2}} \end{cases}, \tag{15}$$

where ρ is the correlation coefficient between the two random variables [$\log(\Delta K_{th})$ and $\log(\Delta \sigma_f)$]. $\rho = 0$ indicates that these two random variables are uncorrelated and $\rho = 1$ indicates that they are fully correlated to each other. The actual value of ρ should be between zero and unity. $\rho = 0$ gives a slightly conservative probabilistic life prediction and is used in this study.

Finally, the mean and standard deviation of EIFS (a) are obtained as

$$\begin{cases} \mu = e^{(\mu_L + \frac{1}{2}\sigma_L^2)} \\ \sigma = [e^{2\mu_L + \sigma_L^2} (e^{\sigma_L^2} - 1)]^{\frac{1}{2}} \end{cases} \tag{16}$$

Eqs. (12)–(16) is the proposed methodology to calculate the statistics of EIFS.

3. Probabilistic life prediction

3.1. Uncertainty quantitation of material crack growth rate

In order to predict material fatigue life (time to failure), the material fatigue crack growth property is required. The first step of probabilistic fatigue life prediction is to quantitate the statistics of the material fatigue crack growth property. A generalized Paris law is used to describe the relationship between da/dN and ΔK and can be expressed as

$$da/dN = C \Delta K^n \left(1 - \frac{\Delta K_{th}}{\Delta K}\right)^p, \tag{17}$$

where C , n , p and ΔK_{th} are fitting parameters. n controls the slope in the Paris regime and p controls the curvature in the near-threshold regime. Eq. (17) only includes near-threshold crack growth and ignores unstable crack growth. For the high-cycle fatigue problem of smooth specimen, ignoring unstable crack growth part will not result in significant error, because most of the fatigue life is spent in the near-threshold crack growth.

Eq. (17) has four parameters to be determined, i.e. C , n , p and ΔK_{th} . It is difficult to determine the statistics of these four parameters simultaneously. In the current study, exponents n and p are assumed to be constants. The randomness in the crack growth is represented by two random variables C and ΔK_{th} . These two random variables are assumed to be independent as the failure mechanisms at the Paris regime and the near-threshold regime are usually different. The fitting procedure is described below.

First, the statistics of ΔK_{th} are quantified. The mean and variance are calculated using crack growth data at very low crack growth rate. The data is fitted to a lognormal distribution. Next, the value of p is determined by fitting crack growth data in the near-threshold regime. Since data points at the near-threshold regime are usually not sufficient to best quantitate the value of p , an initial guess of p was made to facilitate the fitting procedure. Several typical values of p can be found in the NASGRO material database [29], such as 0.25, 0.5, 0.75 and 1. These values are checked and the best regression value is used. Following this, C and n are fitted with experimental data in the Paris regime using the least squares method. The last step is to quantitate the statistics of C using a point-to-point approach. For each data point, the C value is calculated using Eq. (17) and the previously obtained values of n , p and ΔK_{th} (mean value). All the calculated C values are fitted to a distribution. It is found that the lognormal distribution is appropriate for the materials investigated in this paper. An example of fitting results for one type of aluminum alloy $AlSi_9Cu_3$ [30] is shown in Fig. 5, and is used for fatigue life prediction in the next section. It is seen that most of the experimental data falls within the 90% confidence bounds using the proposed uncertainty quantitation method.

3.2. Probabilistic crack growth analysis

Once all the statistics associated with material properties have been quantified, probabilistic life prediction can be performed next. Eq. (17) is rewritten as

$$dN = \frac{1}{C\Delta K^n \left(1 - \frac{\Delta K_{th}}{\Delta K}\right)^p} da \tag{18}$$

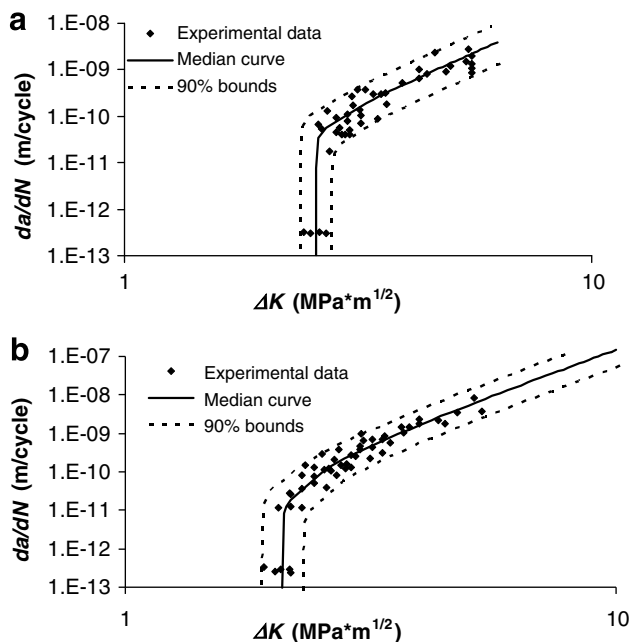


Fig. 5. Crack growth data and uncertainty quantitation for $AlSi_9Cu_3$ (a) 20 °C and (b) 150 °C.

Integrating both sides, fatigue life N can be obtained as

$$N = \int_0^N dN = \int_{a_i}^{a_c} \frac{1}{C\Delta K^n \left(1 - \frac{\Delta K_{th}}{\Delta K}\right)^p} da, \tag{19}$$

where a_i is EIFS determined in the Section 2. a_c is the critical length at failure and can be calculated using fracture toughness and applied stress levels. a_c also depends on the specimen geometry and loading types. For the high-cycle fatigue problem, time spent at fast crack growth regime (regime III) is negligible, and changes in the value of a_c will not affect life prediction significantly. In the current study, a_c is assumed to be a constant. Stress intensity factor range ΔK is calculated as shown in Eq. (7).

The above discussion is for elastic analysis and is appropriate for very high-cycle fatigue analysis, in which materials remain elastic during the entire fatigue life. For medium and low-cycle fatigue problems, materials will experience some plastic deformation. Elastic analysis is not sufficient for fatigue life prediction. For the collected material data in this paper, the shortest fatigue life is in the range of 10^4 cycles. This range is in the transition range from low-cycle fatigue and high-cycle fatigue, where plastic deformation can not be ignored. To include the effect of plastic deformation, an elastic–plastic correction factor based on the BCS model [31] is proposed. Wilkinson [32] derived cyclic reversed plastic zone size as

$$\rho = a \left(\sec \frac{\pi \sigma_{max}(1-R)}{4\sigma_y} - 1 \right), \tag{20}$$

where ρ is the plastic zone size using dislocation theory. It should be noted that this result is similar to Dugdale’s model using continuum mechanics with elastic-perfect plasticity model [32]. A modification to Eq. (20) is proposed as

$$\rho = a \left(\sec \frac{\pi \sigma_{max}(1-R)}{4\sigma_0} - 1 \right), \tag{21}$$

where σ_0 is the flow stress and can be approximated using the material yielding strength σ_y and material ultimate strength σ_u to consider the strain hardening effect as

$$\sigma_0 = \left(\frac{\sigma_y + \sigma_u}{2} \right). \tag{22}$$

Eq. (7) can be expressed considering plasticity correction as

$$\Delta K = \sigma_{max} \sqrt{\pi a'} Y', \tag{23}$$

where Y' is the geometry correction factor using the equivalent crack length a' considering plasticity correction. a' can be expressed as

$$a' = a + \rho. \tag{24}$$

Fatigue life is calculated by combining Eqs. (19) and (23). Numerical integration is performed using an adaptive recursive Simpson’s rule [33]. The current plasticity correction is a very simplified model and further improvements may be required. It is found that the current model works well for the materials investigated. To show the effects of plasticity correction factor, a comparison using pure elastic analysis (Eq. (7)) and elastic–plastic analysis (Eq. (23)) is plotted in Fig. 6. In Fig. 6, solid lines are median curve prediction using elastic–plastic analysis and dashed lines are median curve prediction using elastic analysis. It can be seen that elastic analysis overestimates fatigue life at higher stress amplitude. At lower stress amplitude, the two approaches give almost identical prediction.

In Eq. (19), a_i , C , and ΔK_{th} are random variables. Thus, fatigue life N is also a random variable. The analytical solution for the distribution of N is hard to obtain. Monte Carlo simulation is used to calculate the probabilistic fatigue-life distribution in this study.

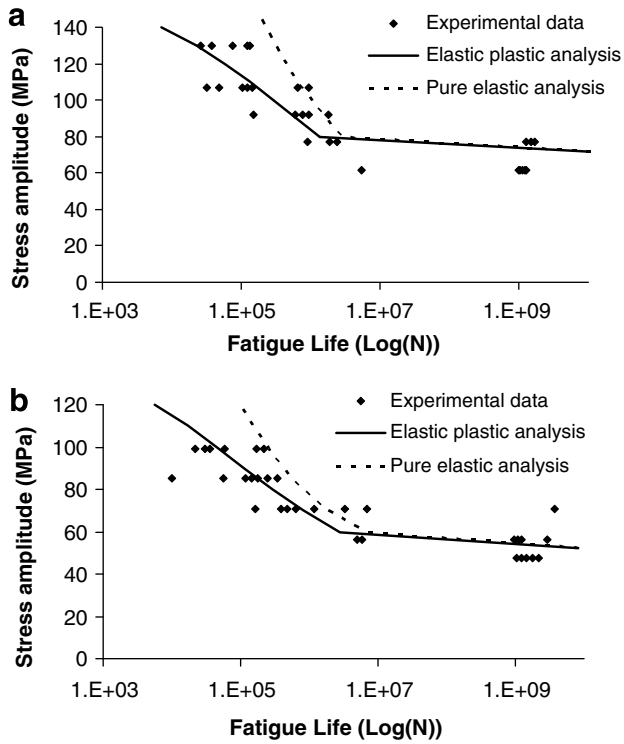


Fig. 6. Comparison between elastic and elastic–plastic analysis for AlSi₉Cu₃ (a) 20 °C and (b) 150 °C.

4. Model validation with experimental data

Several experimental data sets available in the literature are collected and used to validate the proposed methodology for probabilistic EIFS calculation and fatigue life prediction. These materials include: (1) aluminum alloys AlSi₉Cu₃, magnesium alloys AZ91 hp

and AS21 hp at two temperatures reported by Mayer et al. [30]; and (2) aluminum 7075-T6 data under stress ratio $R = -1$ reported by Wang et al. [34]. The mechanical properties required in the proposed methodology are listed in Tables 1–4. The EIFS value reported here is assumed to be for a center-through crack. Experimental data and numerical predictions are shown in Fig. 7 for the collected materials. In Fig. 7, the solid line is the median prediction and dashed lines are 90% confidence bounds using the proposed methodology. It is shown that the prediction results agree with experimental data very well for both trend and scatter.

5. Discussion

Several concerns using the proposed methodology are discussed here and illustrated using the collected experimental data.

5.1. EIFS using assumptions of through crack and surface crack

The proposed EIFS calculation depends on the assumption of the crack configuration as we have shown in Section 2. If a different crack configuration is assumed, the EIFS is usually different since the stress intensity factor solution is different. However, this difference will not change the fatigue life prediction as long as the crack growth analysis uses the same crack configuration. Fig. 7 shows the fatigue life prediction using the center-through crack assumption. We also calculate the fatigue life prediction using the semi-circular surface crack assumption. The other mechanical parameters remain the same. The prediction results are shown in Fig. 8 together with experimental data. Comparing Figs. 7 and 8, the fatigue life predictions are almost the same using two different assumptions, with a few exceptions. The reason is that the proposed EIFS calculation includes the effects of the initial crack configuration (see Eq. (8)). The center-through crack assumption makes the calculation easy to perform and is suitable for fatigue life prediction of the smooth plate specimen in the current investigation. However, the surface crack assumption is closer to the actual situation for structural components. Also, the surface crack assumption can easily be

Table 1
Mechanical properties for AlSi₉Cu₃ aluminum alloy

	150 °C			20 °C		
	Mean	Std.	Distribution	Mean	Std.	Distribution
Yielding strength (MPa)	123	0		134	0	
Ultimate strength (MPa)	198	0		216	0	
C (m/cycle)	6.64E-12	3.78E-12	Lognormal	1.79E-12	1.10E-12	Lognormal
n	4.469	0		4.2511	0	
$K_{max}(R = -1)$ (MPam ^{0.5})	2.07	0.12	Lognormal	2.57	0.12	Lognormal
$\Delta\sigma_f$ (MPa)	61	12	Lognormal	75	14	Lognormal
p	0.75	0		0.25	0	
EIFS a (mm)	0.37	0.14	Lognormal	0.32	0.13	Lognormal

Table 2
Mechanical properties for magnesium alloys AZ91 hp

	125 °C			20 °C		
	Mean	Std.	Distribution	Mean	Std.	Distribution
Yielding strength (MPa)	93	0		118	0	
Ultimate strength (MPa)	165	0		190	0	
C (m/cycle)	1.63E-10	6.97E-11	Lognormal	2.91E-10	1.71E-10	Lognormal
n	4.181	0		2.7045	0	
$K_{max}(R = -1)$ (MPam ^{0.5})	1.12	0.07	Lognormal	1.41	0.12	Lognormal
$\Delta\sigma_f$ (MPa)	41	7	Lognormal	45	7	Lognormal
p	0.75	0		1.5	0	
EIFS a (mm)	0.22	0.07	Lognormal	0.3	0.1	Lognormal

Table 3
Mechanical properties for magnesium alloys AS21 hp

	125 °C			20 °C		
	Mean	Std.	Distribution	Mean	Std.	Distribution
Yielding strength (MPa)	65	0		84	0	
Ultimate strength (MPa)	103	0		131	0	
C (m/cycle)	4.78E-10	2.67E-10	Lognormal	3.15E-10	1.24E-10	Lognormal
n	2.24	0		2.7187	0	
$K_{\max}(R = -1)$ (MPam ^{0.5})	1.05	0.09	Lognormal	1.36	0.11	Lognormal
$\Delta\sigma_f$ (MPa)	27	5	Lognormal	38	8	Lognormal
p	0.75	0		1.5	0	
EIFS 2a (mm)	0.43	0.18	Lognormal	0.41	0.2	Lognormal

Table 4
Mechanical properties for 7075-T6 aluminum alloy

	R = -1		
	Mean	Std.	Distribution
Yielding strength (MPa)	691	0	
Ultimate strength (MPa)	764	0	
C (m/cycle)	6.54E-13	4.01E-13	Lognormal
n	3.8863	0	
ΔK_{th} (MPam ^{0.5})	5.66	0.268	Lognormal
$\Delta\sigma_f$ (MPa)	201	20.1	Lognormal
p	0.75	0	
EIFS a (mm)	0.23	0.05	Lognormal

extended to include notch effects, i.e. using the stress intensity factor solution considering notch effect [26]. It is expected that the surface crack assumption is more suitable for structural level fatigue life prediction.

5.2. Fatigue life prediction for surface crack and internal crack

To better show the proposed method's performance with respect to probabilistic life prediction, cumulative distribution function (CDF) curves constructed using Monte Carlo simulation results are compared with experimental data for aluminum alloys AlSi₉-Cu₃ at two stress levels and under two temperatures. One is under 150 °C and at the stress amplitude of 71 MPa. Another comparison is shown under 20 °C and at the stress amplitude of 107 MPa. CDF curves from experimental data and Monte Carlo simulation are plotted together in Fig. 9. Two basic statistical goodness-of-fit results of the model prediction and experimental observations are performed. Correlation of coefficients are calculated to be 0.96 and 0.95 for Fig. 9a and b, respectively. Nonparametric Kolmogorov–Smirnov test is also performed. The result showed that the test can not reject the null hypothesis at the 5% significance level. The test statistics are 0.22 and 0.25 for Fig. 9a and b, respectively.

From Fig. 9, it is seen that numerical predictions agree with experimental data well. However, at the long life tail region, a small difference can be observed. This phenomenon is discussed below.

From Fig. 9, the experimental data seems to be a bi-modal distribution, with the long life tail appearing to follow another type of CDF. This indicates that another type of failure mechanism is ignored in the numerical prediction. Surface crack is assumed in the probabilistic crack growth analysis and no internal crack growth is assumed. It is known that internal crack is less dangerous compared to the surface crack and may contribute to the long life tail. To justify this statement, a modification of the developed probabilistic crack growth methodology is proposed and validated.

There are two reasons for longer fatigue life of internal cracks. First, the stress intensity factor of embedded cracks is about 10% less compared to surface cracks [25]. Eq. (14) is modified to include a reduction factor of internal cracks as

$$\Delta K = \zeta \sigma_{\max} \sqrt{\pi a'} Y', \quad (25)$$

where ζ is equal to 1 for surface crack and is equal to 1/1.12 for internal cracks. Another reason for longer life of internal crack growth is due to the constraint effects (i.e., plane stress or plane strain) near the crack tip. The constraint effect affects the plastic zone size and the equivalent crack length in the proposed calculation methodology. To include the constraint effects, Eq. (21) is modified as

$$\rho = \frac{1}{\eta} a \left(\sec \frac{\pi \sigma_{\max} (1-R)}{4 \sigma_0} - 1 \right), \quad (26)$$

where η is a correction factor considering constrain effects. $\eta = 1$ for plane stress condition, and $\eta = 3$ for plane strain conditions. A surface crack can be treated as under purely plane stress condition. An embedded crack in an infinite body can be treated as under purely plane strain condition. For an internal crack in a finite thickness plate, it is usually under the condition between purely plane stress and purely plane strain and η takes a value between 1 and 3. In the current investigation, η is assumed to be 2 for the investigated smooth plate specimen. A detailed study of constraint effect may be required for other types of specimens or components.

Following the same procedures described for surface crack growth, probabilistic life prediction can be obtained for internal crack growth. Comparisons with experimental data and previous life prediction assuming surface crack growth are shown in Fig. 10.

From Fig. 10, it is seen that the internal crack growth mechanism can explain the tail shape of probabilistic life distribution. For short fatigue life, surface crack growth predictions agree with experimental data well. For long fatigue life, internal crack growth predictions agree with experimental data well. The actual fatigue-life distribution is a combination of those two predictions for the current investigation. For fatigue reliability analysis, low failure probability or high reliability (e.g., 99% reliability or 1% failure probability) is more important and the short life regime should be the area of interest. If the majority of failure is dominated by the surface crack, which is more dangerous than internal crack growth, probabilistic life prediction based on surface crack assumption is sufficient and will give a slightly conservative prediction.

In the current discussion, no effect of the vacuum effect on the internal crack is included. The longer fatigue life of an internal growing crack is explained by constraints effect. Further study for other materials are required to understand the mechanism of an internal growing crack.

5.3. EIFS and actual initial flaw size

The proposed EIFS methodology presents an equivalent quantity to predict fatigue life using long crack growth data. It does not represent the actual material defect size. However, if the mate-

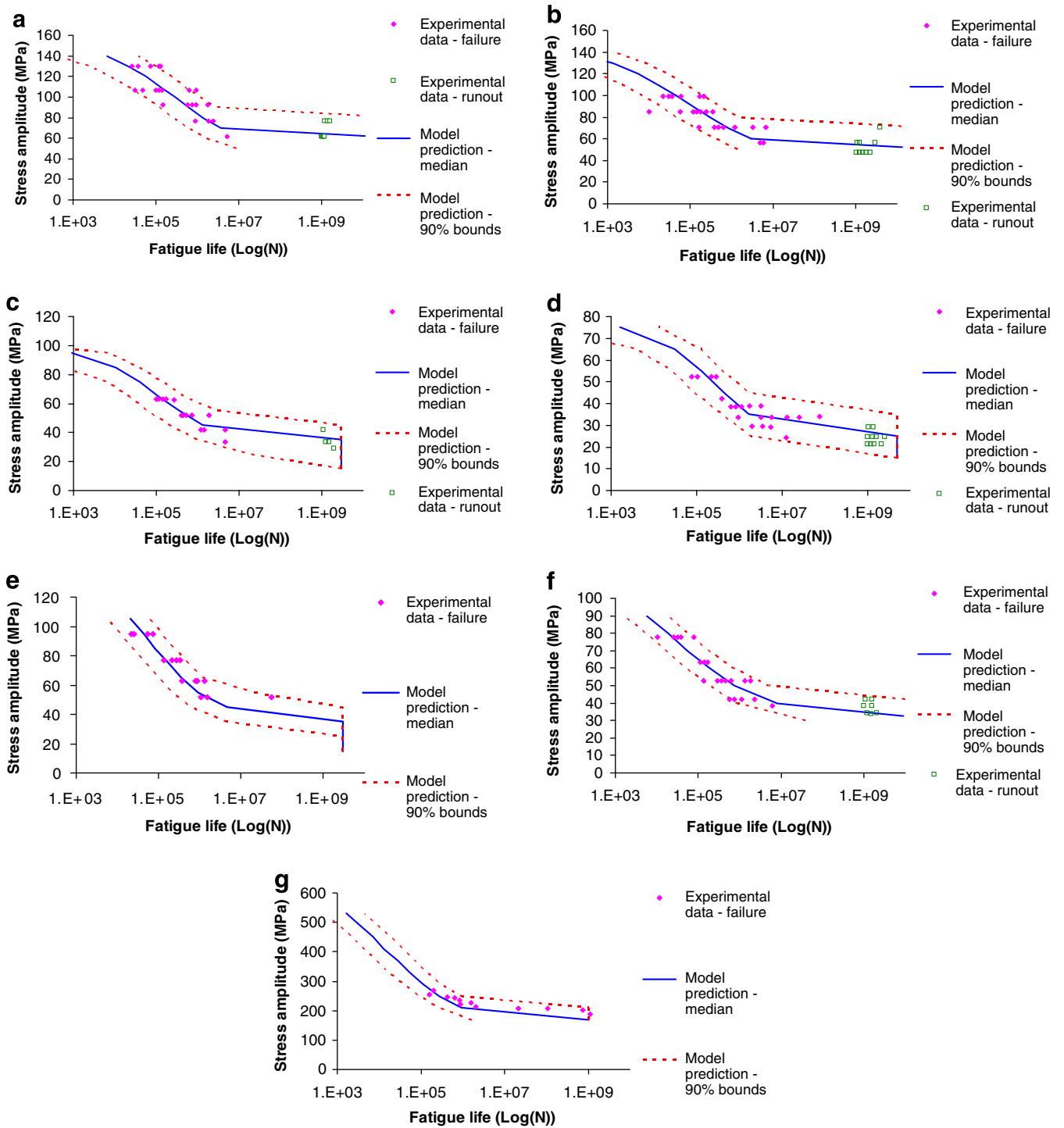


Fig. 7. Comparison between numerical simulation and experimental results for (a) $AlSi_9Cu_3$ at 20 °C; (b) $AlSi_9Cu_3$ at 150 °C; (c) AS21 hp at 20 °C; (d) AS21 hp at 125 °C; (e) AZ91 hp at 20 °C; (f) AZ91 hp at 125 °C; and (g) 7075-T6 at $R = -1$. – Center-through crack assumption.

rial does have large initial flaws, the proposed EIFS could give an estimation of the actual initial flaw size. The reason is that no small-crack growth exists for this type of material. From Fig. 2, we can expect that the proposed EIFS will approach actual initial flaw size when small-crack growth can be ignored (i.e., the area under the small-crack growth curve approaches zero). To justify this statement, measured initial defect sizes (porosities in the reported data) using SEM of aluminum alloys $AlSi_9Cu_3$ and magnesium alloys AZ91 hp are shown in Fig. 11 by plotting their cumulative probability distribution together along with the predicted

EIFS distribution. It is seen that the EIFS predictions using the proposed method agree with experimentally measured defect sizes for $AlSi_9Cu_3$ and deviates from the actual defect size of AZ91. For aluminum 7075-T6, the difference of the EIFS and the actual defect size could be huge. The actual initial flaw size of aluminum 7075 is usually very small and is in the range of 10–20 μm [20]. The calculated EIFS is in the range of 200–300 μm (see Table 4). Generally speaking, the proposed EIFS does not represent the actual initial flaw size and only supplies an initial crack length quantitate for the purpose of life prediction.

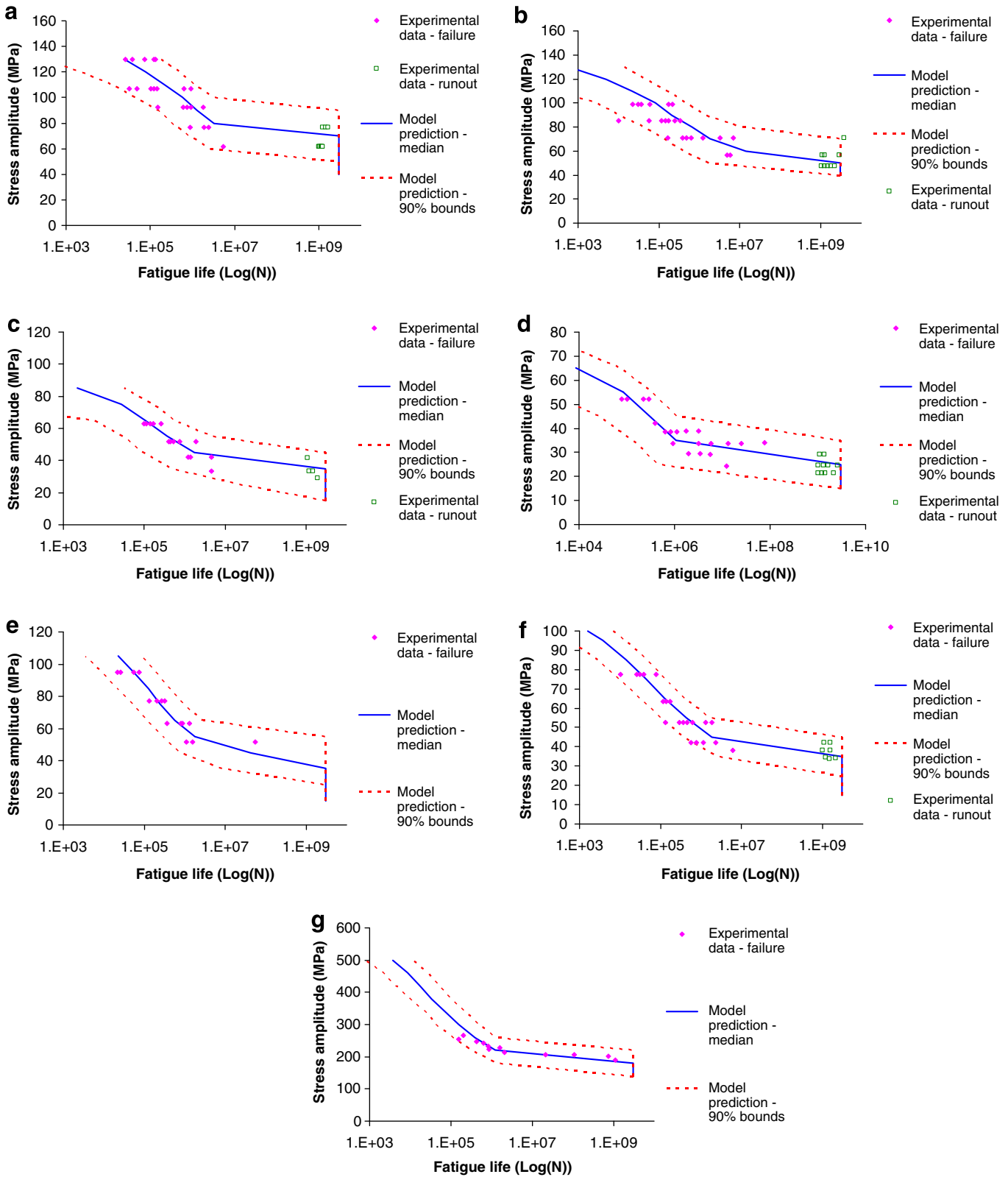


Fig. 8. Comparison between numerical simulation and experimental results for (a) AlSi₉Cu₃ at 20 °C; (b) AlSi₉Cu₃ at 150 °C; (c) AS21 hp at 20 °C; (d) AS21 hp at 125 °C; (e) AZ91 hp at 20 °C; (f) AZ91 hp at 125 °C; and (g) 7075-T6 at R = -1. – Semi-circular surface crack assumption.

5.4. Fatigue endurance limit definitions

One important parameter in the proposed methodology is the fatigue endurance limit. For some materials, fatigue endurance limit can be observed in the fatigue S–N testing. For some other

materials, there is no clearly observed fatigue limit, such as aluminum materials. The fatigue strength of this type of material continues to drop as the loading cycles increases. There is argument whether the endurance limit does exist for metallic materials [35]. The choice of fatigue limit value will affect the EIFS calculation

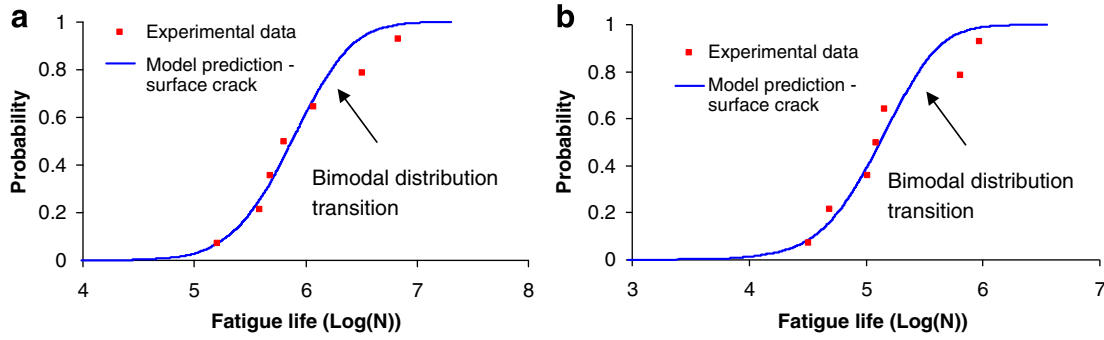


Fig. 9. CDF comparison between numerical simulation and experimental results for AlSi₉Cu₃ (a) S = 71 MPa and temp = 20 °C and (b) S = 107 MPa and temp = 150 °C. Model prediction using surface crack assumption.

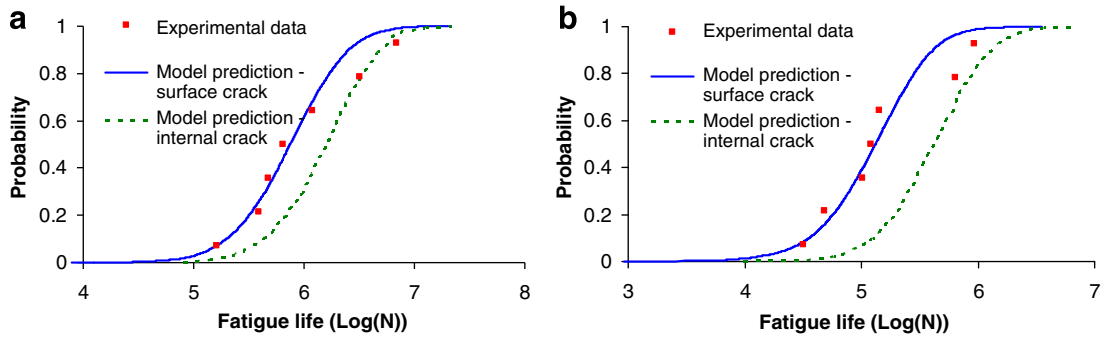


Fig. 10. CDF comparison between numerical simulation and experimental results for AlSi₉Cu₃ (a) S = 71 MPa and temp = 20 °C and (b) S = 107 MPa and temp = 150 °C. Model prediction using both surface crack and internal crack assumption.

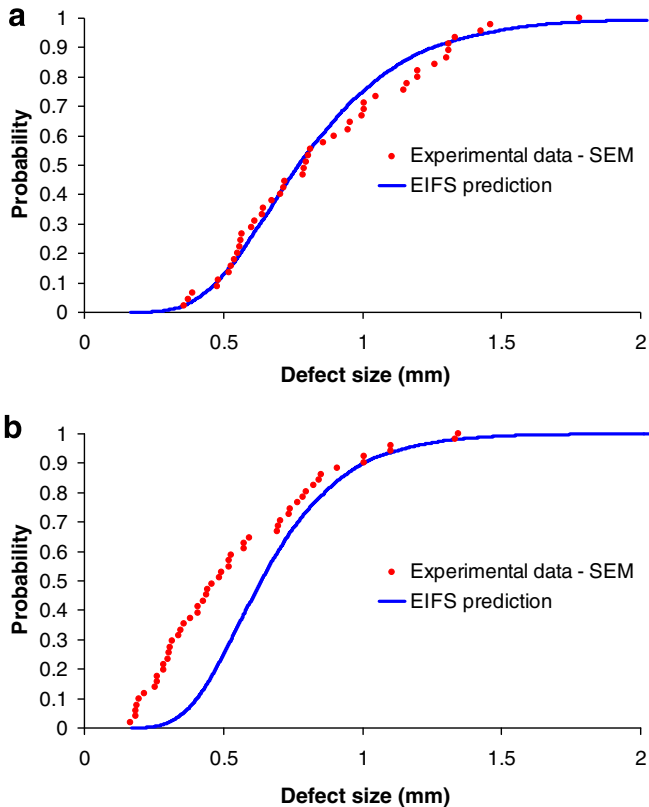


Fig. 11. EIFS prediction and measured initial defects by SEM (a) AlSi₉Cu₃ and (b) AZ91.

and fatigue life prediction. The effect of fatigue limit definition on the proposed methodology is discussed here. For materials that show a fatigue limit in the S–N curve testing, such as AlSi₉Cu₃, AS21, and AZ91 used in this study, fatigue limit distribution can be calculated using the run out experimental data. For materials that do not show fatigue limit behavior in the S–N testing, such as aluminum 7075-T6 used in this study, the fatigue limit value can be defined and estimated using fatigue strength coefficients at very high cycles (i.e., 10⁷–10⁸). Due to the fact that fatigue strength at very high-cycle fatigue regime shows asymptotic behavior, i.e. very small slope in the S–N curve compare to that in the medium-cycle fatigue regime (e.g., 10⁴–10⁶), the different definition of fatigue limit will not lead to a significant difference in the overall fatigue life prediction. Thus the proposed method is still applicable in practical applications. To justify this statement, we show one demonstration example for Al-7075-T6 using different fatigue limit definitions. The first case uses the fatigue strength coefficient interpolated at 10⁷ cycles. The second case uses the fatigue strength coefficient interpolated at 10⁸ cycles. The third case uses the averaged value of fatigue strength coefficients beyond 10⁷ cycles. The model predictions for these three cases are shown in Fig. 12 together with experimental data. It is shown that the fatigue life prediction has no significant difference in the three cases. In the current investigation, the fatigue limit estimation uses the average value of reported fatigue strength coefficients beyond 10⁷ cycles.

5.5. Fatigue crack threshold stress intensity factor measurement

Another important parameter is the fatigue crack threshold stress intensity factor range in the EIFS calculation. It is known that the estimated fatigue crack threshold stress intensity factor range (ΔK_{th}) depends on the experimental procedure. Different experi-

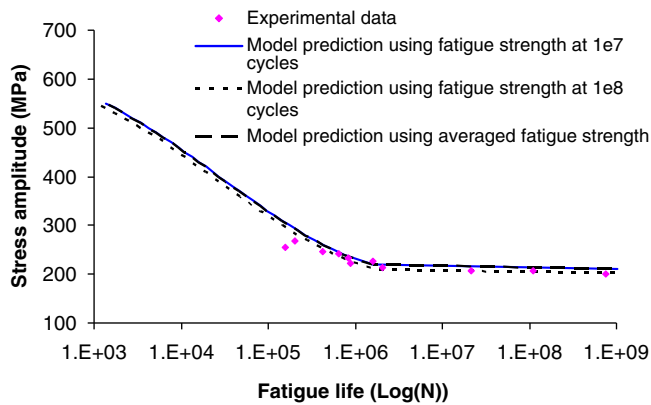


Fig. 12. Fatigue-life prediction using different fatigue limit definitions.

mental techniques will lead to different ΔK_{th} estimates, such as those from load-reduction or compression pre-cracking constant amplitude procedures (CPCA) [36]. The EIFS calculation and fatigue life prediction will depend on the experimental technique used to measure ΔK_{th} . Detailed theoretical and experimental study on the selection and justification of proper experimental techniques in determining the crack threshold stress intensity factor range is beyond the scope of this study. In the current investigation, the ΔK_{th} of the collected experimental data [30,34] is measured using piezoelectric ultrasonic resonance testing at about 20 kHz. This method is originally proposed by Mayer et al. [30], which is different from the typically used load-reduction or CPCA technique [36]. In the experimental validation section, it is shown that the proposed methodology and the used ΔK_{th} estimation from this technique give a satisfactory life prediction in the current investigation. The usage of the proposed methodology with ΔK_{th} measured by load-reduction or CPCA needs further study. Another important issue is the data fitting near the near-threshold regime, where experimental data is very hard to obtain. Further investigation is required for near-threshold data fitting.

6. Conclusion

A new probabilistic EIFS calculation methodology is proposed in this paper. Unlike existing back-extrapolation methods for EIFS calculation, the proposed method is based on the Kitagawa–Takahashi diagram and tries to match the infinite fatigue life of specimen by using the fracture mechanics-based life prediction approach. One advantage of the proposed method is that it only requires fatigue limit data and fatigue crack threshold intensity factor data for EIFS calculation, which makes the proposed EIFS is independent of stress levels. The other advantage is that it does not solve the inverse crack growth problem, which makes the calculation of EIFS statistics very efficient. A probabilistic fatigue crack growth analysis based on the EIFS distribution is also proposed to calculate the fatigue life distribution of smooth plate specimens. Plasticity correction is included in the proposed methodology and Monte Carlo simulation is used to calculate the fatigue life distribution using the developed EIFS method. Several experimental data for different metallic materials are used to validate the proposed methodology.

Based on the results of investigated materials, several conclusions can be drawn:

- (1) Through crack and surface crack assumption will obviously offset the results of EIFS using the proposed methodology. However, this change will not affect the probabilistic life prediction, as long as EIFS and life prediction calculation use the same assumption.

- (2) The probabilistic life prediction of aluminum alloys $AlSi_9Cu_3$ under two stress levels and under two temperatures (150 °C and under stress amplitude of 71 MPa; 20 °C and under the stress amplitude of 107 MPa) shows a bi-modal distribution, which can be explained by the presence of both surface crack growth and internal crack growth mechanisms. Surface crack growth contributes to the short life tail and is more critical for fatigue reliability analysis.
- (3) For materials with large initial defects, the proposed EIFS can give a good estimate of the actual material flaw size. For materials with very small initial defects, the proposed EIFS only presents an equivalent quantity for fatigue life prediction using long crack growth data.

The proposed EIFS calculation is validated using smooth plate specimens under constant amplitude loading. Future study is required for notched specimen and under variable amplitude loading. This paper only considered uniaxial Mode I loading. The validity of the proposed method under arbitrary mixed-mode loading needs further study.

Acknowledgements

The research reported in this paper was supported by funds from the Federal Aviation Administration William J. Hughes Technical Center (Contract No. DTFAC-06-C-00017, Project Manager: Dr. Dy Le). The support is gratefully acknowledged.

References

- [1] Joint service specification guide aircraft structures, JSSG-2006. United States of America: Department of Defense; 1998.
- [2] Gallagher JP, G.F., Berens AP, Engle Jr RM, USAF damage tolerant design handbook: guidelines for the analysis and design of damage tolerant aircraft structures? Final report. 1984.
- [3] Merati A, Eastaugh G. Determination of fatigue related discontinuity state of 7000 series of aerospace aluminum alloys. *Eng Failure Anal* 2007;14(4):673–85.
- [4] Krasnowski BR, Rotenberger KM, Spence WW. A damage-tolerance method for helicopter dynamic components. *J Am Helicopter Soc* 1991;36(2).
- [5] Forth SC, Everett Jr RA, Newman JA. A novel approach to rotorcraft damage tolerance. 6th Joint FAA/DoD/NASA aging aircraft conference. 2002.
- [6] Yang JN, M.S. Distribution of equivalent initial flaw size. In: Proceedings of the annual reliability and maintainability symposium. San Francisco (CA): 1980.
- [7] White P, Molent L, Barter S. Interpreting fatigue test results using a probabilistic fracture approach. *Int J Fatigue* 2005;27(7):752–67.
- [8] Molent L, Sun Q, Green A. Characterisation of equivalent initial flaw sizes in 7050 aluminium alloy. *J Fatigue Fract Eng Mater Struct* 2006;29:916–37.
- [9] Moreira PMGP, de Matos PFP, de Castro PMST. Fatigue striation spacing and equivalent initial flaw size in Al 2024-T3 riveted specimens. *Theor Appl Fract Mech* 2005;43(1):89–99.
- [10] Fawaz SA. Equivalent initial flaw size testing and analysis; 2000.
- [11] Cross R, Makeev A, Armanios E. Simultaneous uncertainty quantification of fracture mechanics based life prediction model parameters. *Int J Fatigue* 2007;29(8):1510–15.
- [12] Makeev A, Nikishkov Y, Armanios E. A concept for quantifying equivalent initial flaw size distribution in fracture mechanics based life prediction models. *Int J Fatigue* 2007;29(1):141–5.
- [13] Lankford J, Hudak SJ. Relevance of the small crack problem to lifetime prediction in gas turbines. *Int J Fatigue* 1987;9(2):87–93.
- [14] Kaynak C, Ankara A, Baker TJ. A comparison of short and long fatigue crack growth in steel. *Int J Fatigue* 1996;18(1):17–23.
- [15] Donnelly E, Nelson D. A study of small crack growth in aluminum alloy 7075-T6. *Int J Fatigue* 2002;24(11):1175–89.
- [16] Xue Y et al. Microstructure-based multistage fatigue modeling of a cast AE44 magnesium alloy. *Int J Fatigue* 2007;29(4):666–76.
- [17] Wang L et al. Three dimensional finite element analysis using crystal plasticity for a parameter study of microstructurally small fatigue crack growth in a AA7075 aluminum alloy. *Int J Fatigue*, in press, doi: 10.1016/j.ijfatigue.2008.03.027.
- [18] Potirniche GP, Daniewicz SR. Finite element modeling of microstructurally small cracks using single crystal plasticity. *Int J Fatigue* 2003;25(9–11):877–84.
- [19] Lukas P, Kunz L. Small cracks – nucleation, growth and implication to fatigue life. *Int J Fatigue* 2003;25(9–11):855–62.
- [20] Newman JC, Phillips EP, Swain MH. Fatigue-life prediction methodology using small-crack theory. *Int J Fatigue* 1999;21(2):109–19.

- [21] Park JS et al. A microstructural model for predicting high cycle fatigue life of steels. *Int J Fatigue* 2005;27(9):1115–23.
- [22] Liu Y, Stratman LL, Mahadevan S. Multiaxial fatigue reliability analysis of railroad wheels. *Reliab Eng Syst Safe* 2008;93(3):456–67.
- [23] Kitagawa H, Takahashi S. Applicability of fracture mechanics to very small cracks or cracks in early stage. In: *Proceedings of the 2nd international conference on mechanical behavior of materials*. USA (OH): ASM International; 1976.
- [24] El Haddad MH, Topper TH, Smith KN. Prediction of nonpropagating cracks. *Eng Fract Mech* 1979;11:573–84.
- [25] Anderson TL. *Fracture mechanics: fundamentals and applications*. CRC Press; 1995.
- [26] Jones R et al. Weight functions, CTOD, and related solutions for cracks at notches. *Eng Failure Anal* 2004;11(1):79–114.
- [27] Newman JCRI, Raju IS. Stress-intensity factor equations for cracks in three-dimensional finite bodies subjected to tension and bending loads. In: Atluri Satya N, editor. *Computational methods*. Elsevier Science; 1986. p. 312–34.
- [28] Maymon G. Probabilistic crack growth behavior of aluminum 2024-T351 alloy using the 'unified' approach. *Int J Fatigue* 2005;27(7):828–34.
- [29] NASA. *Fatigue crack growth computer program NASGRO version 3.0 – reference manual*. Texas: NASA, Lyndon B, Johnson Space Center; 2000.
- [30] Mayer H, Papakyriacou M, Zettla B, Vacić S. Endurance limit and threshold stress intensity of die cast magnesium and aluminum alloys at elevated temperatures. *Int J Fatigue* 2005;27:1076–88.
- [31] Bilby BA, Cottrell AH, Swinden KH. The spread of plastic yield from a notch. *Proc Roy Soc London Set A* 1963;272:304–14.
- [32] Wilkinson AJ. Modelling the effects of texture on the statistics of stage I fatigue crack growth. *Phil Mag A* 2001;81:841–55.
- [33] Gander W, Gautschi W. Adaptive quadrature – revisited. *BIT* 2000;40:84–101.
- [34] Wang QY, Kawagoishi N, Chen Q. Fatigue and fracture behavior of structural Al-Alloy up to very long life regimes. *Int J Fatigue* 2006;28:1572–6.
- [35] Bathias C. There is no infinite fatigue life in metallic metals. *Fatigue Fract Eng Mater Struct* 1999;22:559–65.
- [36] Newman Jr J, Schneider J, Daniel A, McKnight D. Compression pre-cracking to generate near threshold fatigue-crack-growth rates in two aluminum alloys. *Int J Fatigue* 2005;27:1432–40.